Solid State Phenomena
ISSN: 1662-9779, Vol. 390, pp 111-119
doi:10.4028/p-os8U1C

Submitted: 2026-01-19
Revised: 2026-02-20
Accepted: 2026-02-21
Online: 2026-04-17

Experimental Study on the Relationship between Cooling Rate, Secondary Dendrite Arm Spacing and Tensile Properties in Aluminum Casting

Taegyun Ahn[1,a], Juwon Lee[1,b], Janghoon Lee[2,c] and Jeong Whan Yoon[1,3,d*]

[1]Department of Mechanical Engineering, Korea Advanced Institute of Science and Technology (KAIST), 291 Daehak-ro, Yuseong-gu, Daejeon 34141, Republic of Korea

[2]Manufacturing Solution Division, Hyundai Motor Group, 37 Cheoldobangmulgwan-ro, Uiwang-si, Gyeonggi-do 06797, Republic of Korea

[3]School of Engineering, Deakin University, 75 Pigdons Rd., Waurn Ponds, VIC 3216, Australia

[a]t.ahn@kaist.ac.kr, [b]juwonlee@kaist.ac.kr, [c]jhlee0212@kia.com, [d]j.yoon@kaist.ac.kr

Keywords: Aluminum casting, Cooling rate, Secondary dendrite arm spacing (SDAS), Mechanical properties, Thermal analysis

Abstract. The dendritic microstructure formed during solidification plays a critical role in determining the mechanical properties of aluminum castings. In particular, secondary dendrite arm spacing (SDAS) is strongly influenced by the cooling rate and is closely related to yield strength, ultimate tensile strength, and elongation. However, experimental validation of these relationships requires a consistent methodology for defining cooling rate and linking it to microstructural and mechanical measurements. In this study, an experimental framework was established to investigate the relationships among cooling rate, SDAS, and mechanical properties in aluminum castings. Casting blocks with different thicknesses were fabricated to obtain a wide range of cooling rates. Cooling curves were measured during solidification, and cooling rates were determined using the second derivatives of the cooling curves. SDAS measurements and tensile tests were conducted on specimens extracted from symmetric positions within the casting blocks to ensure equivalent thermal histories. The results showed that the cooling rate–SDAS relationship exhibited a linear trend on a logarithmic scale, consistent with previously reported correlations. Smaller SDAS values were associated with increased yield strength, ultimate tensile strength, and elongation. The agreement between the present results and literature data confirms the validity of the proposed experimental framework for correlating solidification conditions, microstructure, and mechanical properties of aluminum castings.

1. Introduction

Aluminum castings are widely used in automotive, aerospace, and structural applications due to their low density, good castability, and favorable mechanical performance. The mechanical properties of aluminum castings are strongly governed by the microstructure developed during solidification [1-3]. Among various microstructural parameters, secondary dendrite arm spacing (SDAS) has been recognized as a key indicator of solidification conditions and final material performance [4-6].

It is well established that SDAS decreases with increasing cooling rate, leading to finer microstructures [7, 8] and improved mechanical properties such as yield strength (YS), ultimate tensile strength (UTS), and elongation (El) [9, 10]. Numerous studies have proposed empirical relationships linking cooling rate and SDAS, as well as correlations between SDAS and mechanical properties [11, 12]. Despite these efforts, experimental verification of such relationships remains challenging due to ambiguities in defining cooling rate and difficulties in directly correlating microstructural observations with mechanical test results obtained from the same thermal conditions. One major experimental challenge arises from the fact that cooling curves obtained during casting are often non-ideal, making the determination of representative cooling rates ambiguous. Additionally, it is not always feasible to extract specimens for microstructural analysis and mechanical testing from the exact same location within a casting, which can lead to inconsistencies

in thermal history and data interpretation. These limitations highlight the need for a robust experimental framework that enables consistent evaluation of cooling rate, SDAS, and mechanical properties.

The objective of this study is to establish and validate an experimental methodology for correlating cooling rate, SDAS, and mechanical properties in aluminum casting. By employing casting blocks with different thicknesses, cooling rates were systematically varied and quantified using the second derivatives of cooling curves. SDAS measurements and tensile tests were conducted on specimens extracted from symmetric locations to ensure equivalent thermal histories. The experimental results were analyzed and compared with literature-reported correlations to assess the validity of the proposed framework.

2. Specimen Preparation

Casting Design and Solidification Conditions. To achieve various cooling rates, the casting was designed to have six steps with different thicknesses of 4, 5, 7, 10, 14 and 18 mm, where thinner steps were intended to produce higher cooling rates. A total of seven castings were solidified to ensure repeatability of the experimental data.

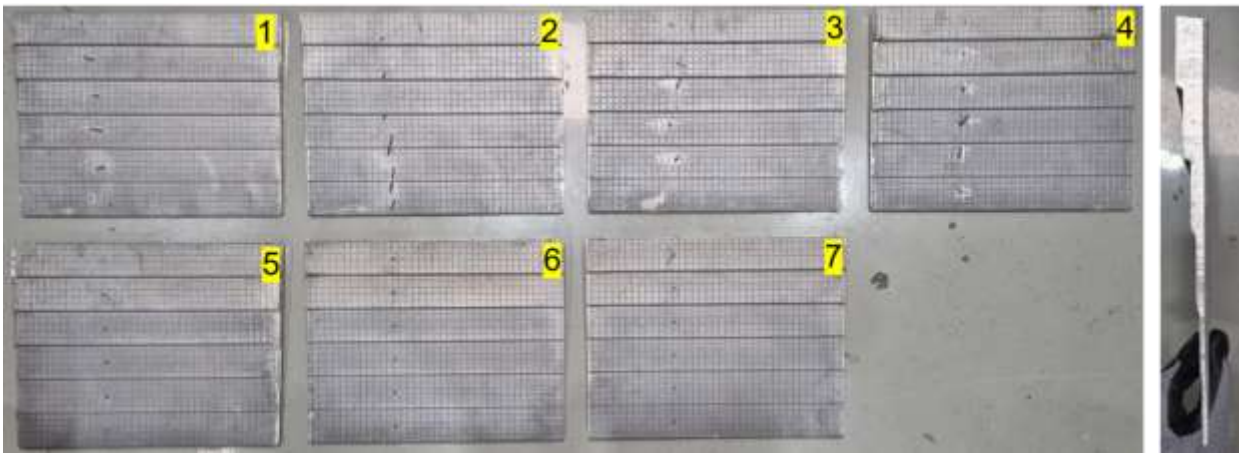

Fig. 1. Aluminum castings with multiple thicknesses

Temperature Measurement and Specimen Location Strategy. To establish correlations between cooling rate, SDAS, and mechanical properties, it is ideally required that thermocouple measurements, SDAS observations, and tensile tests be conducted at the same location. However, this was not feasible for several reasons.

First, tensile specimens could not be extracted from the thermocouple location due to the presence of the thermocouple hole. Second, SDAS observation requires grinding and polishing, which would damage tensile specimens if performed prior to testing. Conversely, performing tensile tests before SDAS observation would deform the dendritic structure, preventing accurate SDAS measurement.

While most of the prior studies do not mention about this problem, a study has addressed this issue by extracting specimens near the thermocouple location or measuring SDAS at the grip region of tensile specimens [11]. However, these approaches may result in discrepancies in thermal history between the gauge region and the thermocouple measurement location.

In this study, thermal symmetry about the center line of the casting was assumed. Thermocouples were placed at a distance of 50 mm from the center line, and SDAS specimens were extracted at the same location. Tensile specimens were extracted from another location 50 mm from the center line on the opposite side, where an identical thermal history was assumed. The validity of this assumption was verified by comparing SDAS values measured at both symmetric locations, which showed good agreement.

Specimen Geometry and Preparation. For SDAS measurement, coin-shaped specimens were fabricated. From the top view, the center of the specimen corresponded to the thermocouple location.

The specimen diameter was 25 mm, which was selected to accommodate grinding and polishing procedures. From the side view, grinding and polishing were performed until the mid-plane along the thickness direction of the casting block was reached, allowing observation of the microstructure at the thickness center.
Tensile specimens were extracted in a similar manner. From the top view, the center of the gauge section coincided with the symmetric position relative to the thermocouple location. From the side view, specimens were extracted from the mid-thickness of the casting blocks.

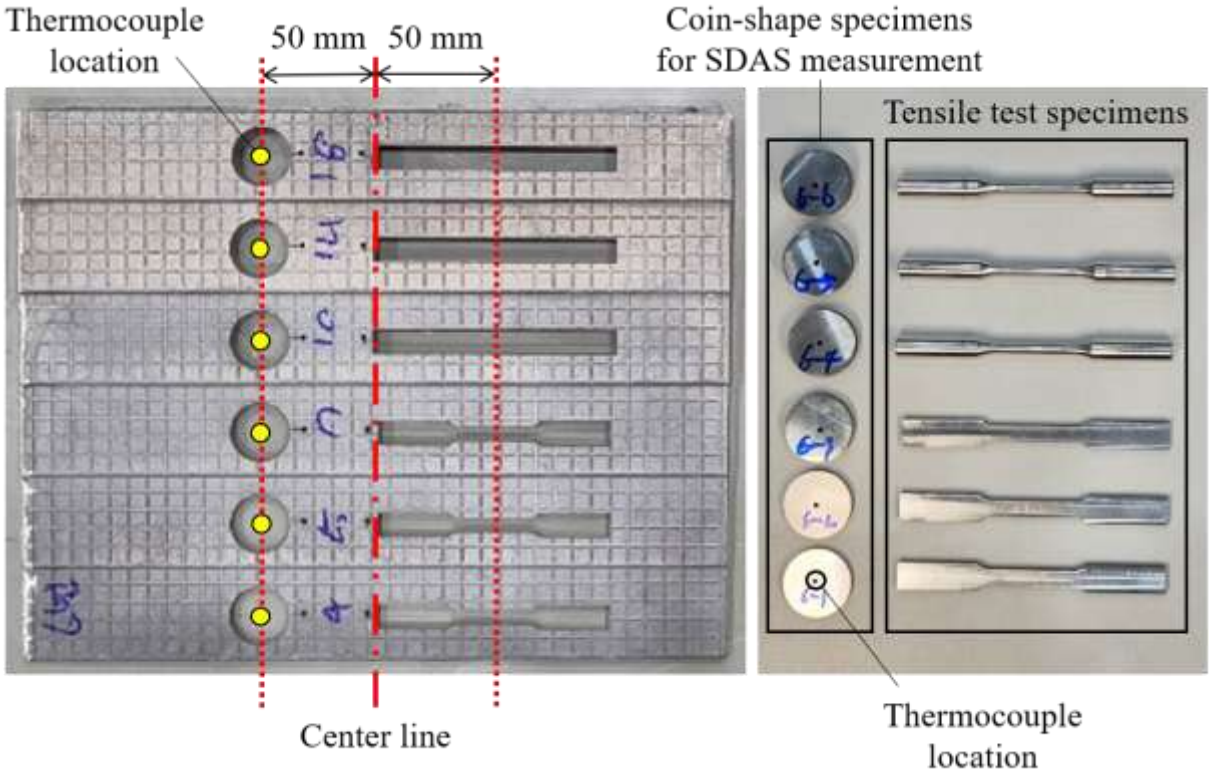

Fig. 2. Locations of thermocouples, specimen extraction positions, and extracted specimens

Tensile Specimen Type Selection. For tensile testing of cast metals, round specimens are commonly used to minimize the influence of non-uniform pore distribution. However, for casting blocks with thicknesses of 4, 5, and 7 mm, the limited thickness made it impractical to fabricate round specimens. Therefore, flat specimens were employed for these conditions.
Although the combined use of round and flat specimens may raise concerns regarding result comparability, thin casting blocks were required in this study to achieve high cooling rates, making the use of flat specimens unavoidable. While round specimens with reduced gauge diameters could have been extracted, such specimens were expected to be excessively sensitive to porosity, resulting in large scatter and poor repeatability in tensile test results. Consequently, flat specimens were selected to ensure more consistent and reliable mechanical property measurements under high cooling rate conditions.

3. Thermal Analysis

Challenges in Analyzing Non-Ideal Cooling Curves. In an ideal cooling curve, a plateau with zero slope appears during phase transformation, where the temperature remains constant due to the release of latent heat. In practice, however, this plateau often exhibits a finite slope as a result of an imbalance between the rate of latent heat release and the rate of heat loss to the surrounding environment. Furthermore, experimental noise and extremely high cooling rates can obscure subtle slope changes, making it difficult to clearly identify the phase transformation region directly from the cooling curve.

Identification of Phase Transformation using Derivatives. To identify phase transformation under non-ideal cooling conditions, numerical differentiation of the cooling curve was employed. While phase transformation can be inferred from changes in the slope (or first derivative) of the cooling curve, gradual slope variations make it difficult to determine a distinct transformation point. Since the second derivative captures the onset of slope change, it provides a clearer mathematical criterion for detecting phase transformation. Moreover, from a physical standpoint, the release of latent heat during phase transformation reduces the cooling rate, resulting in a pronounced response in the second derivative. Previous studies have also reported that using the second derivative provides a more reliable criterion for identifying the onset of phase transformation [13, 14]. Accordingly, the second derivative of the cooling curve was used to identify phase transformation regions in this study.
The material investigated was an Al–Si alloy, in which primary α-Al solidifies first, followed by eutectic Si. Therefore, the first peak in the second derivative was defined as the onset of primary α-Al solidification, and the second peak as the onset of eutectic silicon solidification.

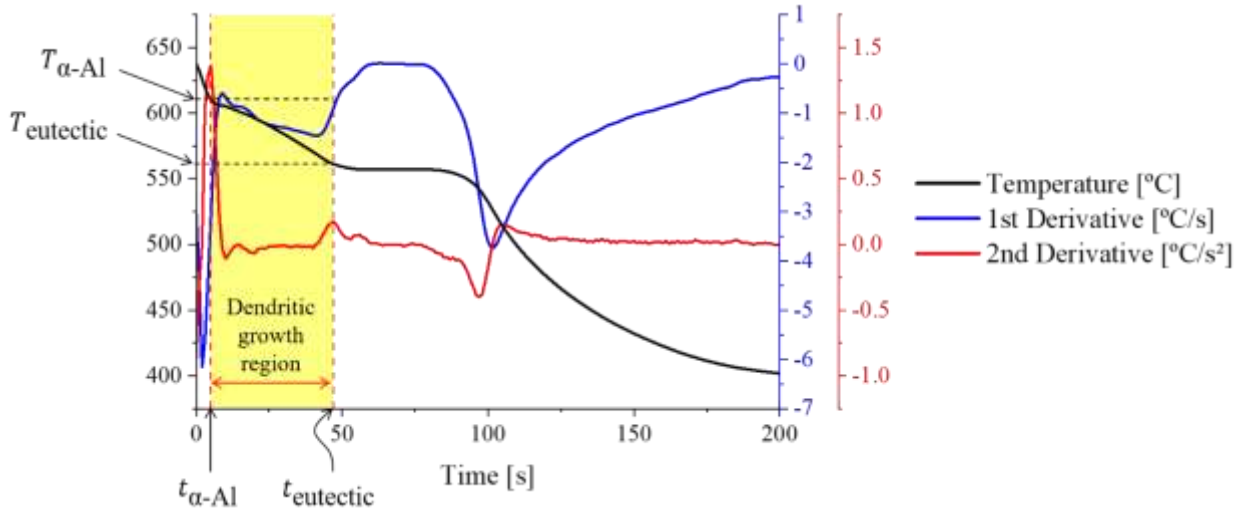

Fig. 3. Identification of the dendritic growth region based on the second derivative of the cooling curve

Average Cooling Rate over Dendritic Growth Region. Once the phase transformation interval was identified, the average cooling rate relevant to SDAS formation was calculated. Previous studies have shown that dendritic growth becomes negligible after the onset of eutectic Si solidification, and thus SDAS is not expected to change beyond this point [15, 16]. Based on this assumption, the dendritic growth interval was defined as the temperature range between the onset of primary α-Al solidification and the onset of eutectic Si solidification [8, 17]. The average cooling rate was calculated over this interval and used for correlation with SDAS.

$$\text{Average Cooling Rate} = \frac{T_{\alpha\text{-Al}} - T_{\text{eutectic}}}{t_{\text{eutectic}} - t_{\alpha\text{-Al}}} \quad (1)$$

For the 4 mm thick casting block, solidification of primary α-Al began before the molten metal fully filled the mold, making it impossible to directly identify the onset of α-Al solidification from the cooling curve. Consequently, the average cooling rates obtained from other block thicknesses were fitted using an exponential function, and the extrapolated value was adopted as the average cooling rate for the 4 mm block. This exponential fitting was used solely for estimating the cooling rate of the 4 mm block. For blocks with well-defined average cooling rates, the experimentally determined values were directly used, together with the measured SDAS, to establish the relationship between SDAS and average cooling rate.

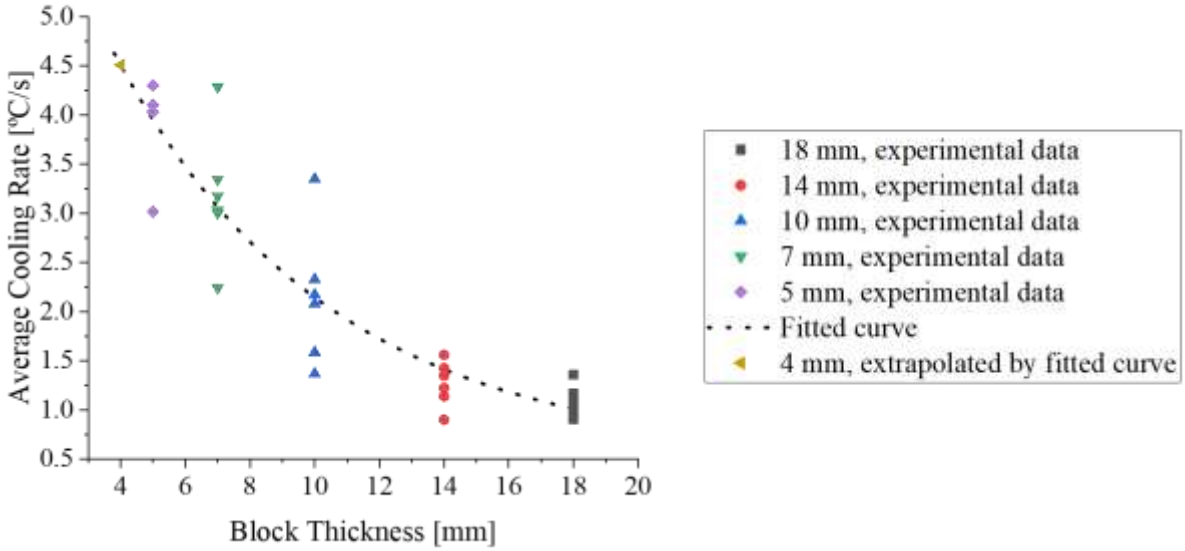

Fig. 4. Measured average cooling rates according to the block thicknesses

4. Results and Discussion

Relationship between SDAS and Average Cooling Rate. The dendritic microstructures were observed near the thermocouple locations using optical microscopy, as shown in Fig. 5. A clear difference in microstructural scale was observed depending on the casting block thickness, and consequently on the cooling rate. SDAS was measured using the linear intercept method [18], which is widely adopted for SDAS evaluation. The measured SDAS values are plotted as a function of average cooling rate in Fig. 6.

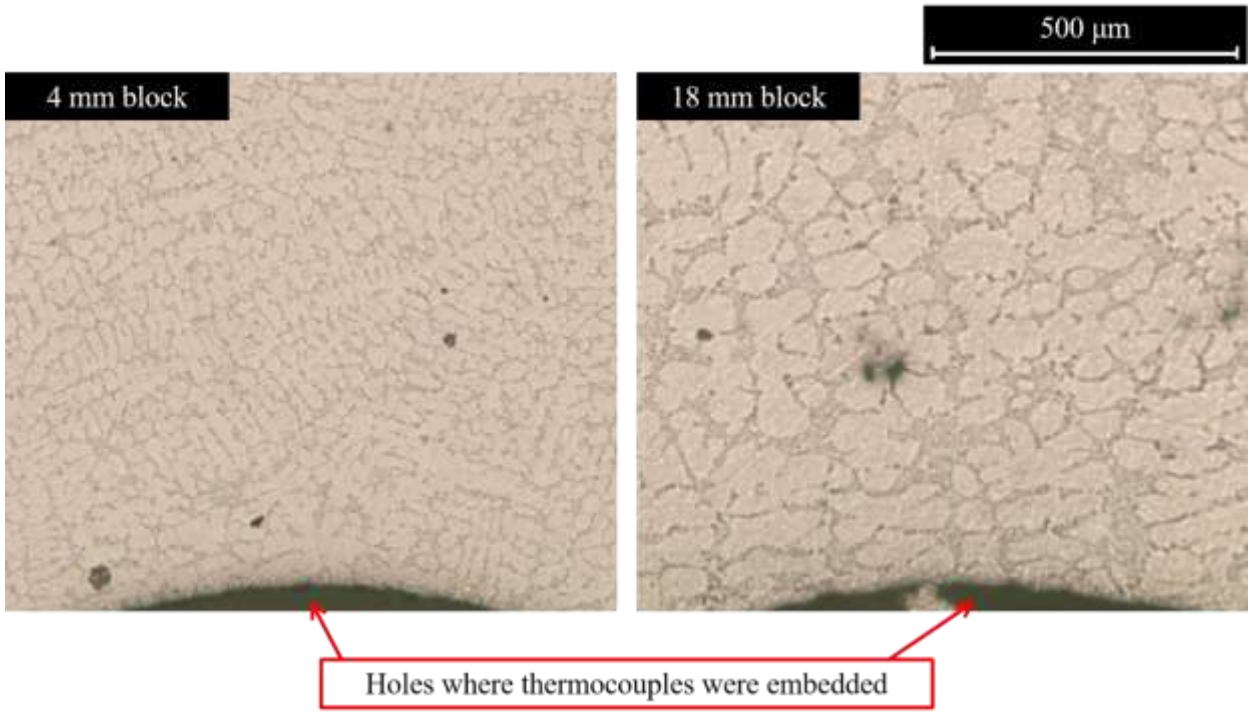

Fig. 5. Optical micrographs showing dendritic microstructures in 4 mm and 18 mm casting blocks near thermocouple location

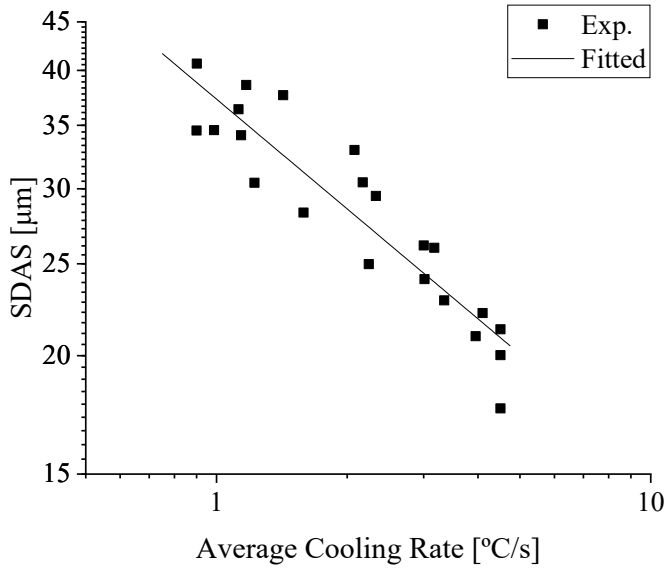

Fig. 6. SDAS versus average cooling rate with fitted curve

The relationship between SDAS and average cooling rate is commonly described by a linear fit on a log–log scale. Accordingly, in the present study, the experimental data were fitted using the power-law:

$$\mathrm{SDAS} = b(\mathrm{AC})^{-n} \tag{2}$$

where $b = 37.303\ \mu\mathrm{m}\cdot(^{\circ}\mathrm{C/s})^{0.385}$, $n = 0.385$ and AC denotes the average cooling rate. The obtained exponent n falls within the range of 1/3 to 1/2 reported by Flemings [7], indicating that the experimental procedure and data analysis employed in this study are consistent with established literature.

It should be noted that some scatter is present in the SDAS measurements, which can be attributed to local variations in dendritic morphology and inherent uncertainties associated with the linear intercept method. Nevertheless, the overall trend of decreasing SDAS with increasing cooling rate is clearly observed, and the fitted relationship captures the experimental data well. This result suggests that the SDAS measurements obtained in this study are sufficiently reliable for establishing quantitative correlations with cooling rate and mechanical properties.

SDAS Agreement at Symmetric Location. To verify the assumption that symmetric locations with respect to the casting centerline experience identical thermal histories, SDAS measurements were performed at both locations. One location corresponded to the thermocouple position, from which specimens for SDAS observation were extracted, while the other was the symmetric position used for tensile specimen extraction.

Table 1. Comparison of SDAS measured at symmetric locations

Thickness of the block [mm]	SDAS at thermocouple location [μm]	SDAS at the symmetric location [μm]
18	21.4	22.3
14	25.3	25.7
10	28.8	27.5
7	31.4	32.0
5	37.6	34.3
4	46.2	44.5

The measured SDAS values at the two symmetric locations are summarized in Table 1. For all casting block thicknesses examined, the SDAS values measured at the symmetric locations showed good agreement.
These results confirm that the assumption of equivalent thermal histories at symmetric locations is reasonable for the present casting geometry. Accordingly, the tensile specimens extracted from the symmetric positions can be reliably correlated with the SDAS values measured at the thermocouple locations, enabling consistent analysis of the relationships among cooling rate, microstructure, and mechanical properties.

Relationship Between Mechanical Properties and SDAS. Since SDAS measured at symmetric locations showed good agreement, the SDAS obtained at the thermocouple locations was correlated with the mechanical properties measured from tensile specimens extracted from the corresponding symmetric positions. As discussed previously, this approach was established to overcome the experimental limitation that microstructure observation and tensile testing cannot be performed simultaneously on a single specimen. The experimental results and fitted relationships are given in Fig. 7 and Eq. 3 to Eq. 5.

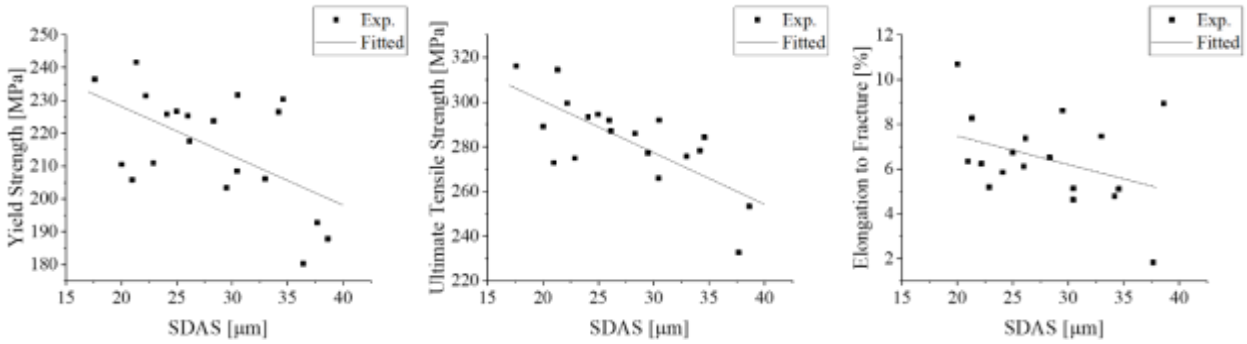

Fig. 7. Mechanical properties versus SDAS with fitted line

$$\text{YS [MPa]} = -1.51(\text{SDAS [μm]}) + 258.27 \quad (3)$$

$$\text{UTS [MPa]} = -2.31(\text{SDAS [μm]}) + 346.64 \quad (4)$$

$$\text{El [\%]} = -0.128(\text{SDAS [μm]}) + 10.04 \quad (5)$$

One limitation of the present study is related to the quality of the casting process. The casting experiments were conducted by a non-specialized casting facility, and as a result, the overall casting quality was not optimal. In particular, a relatively high level of porosity was observed in the castings, which contributed to significant scatter in the measured mechanical properties. Since tensile properties are highly sensitive to porosity, especially elongation, this variability limited the consistency of the experimental data. It is expected that improved control of the casting process, such as optimized melt handling, degassing, and mold design, would reduce porosity and lead to more reliable mechanical property measurements. Therefore, further improvement in casting quality would enable more quantitative and refined correlations between SDAS, and mechanical properties.
Although some scatter was observed in the experimental data, a clear decrease in yield strength (YS) and ultimate tensile strength (UTS) with increasing SDAS was evident. The scatter in elongation (El) to fracture was larger than that in YS and UTS, which can be attributed to the higher sensitivity of elongation to casting porosity and specimen geometry. In particular, the use of both flat and round specimens may complicate direct comparison of elongation. To minimize this effect, the cross-sectional areas of the flat and round specimens were matched as closely as possible. Despite the increased scatter, elongation also exhibited a decreasing trend with increasing SDAS. Overall, all three mechanical properties—YS, UTS, and elongation to fracture—were found to decrease with increasing SDAS. This trend can be explained in terms of microstructure refinement. A smaller SDAS corresponds to a finer dendritic structure, which reduces the effective interdendritic spacing and

restricts dislocation motion, thereby increasing strength. From a ductility standpoint, in fine dendritic structures, interdendritic regions are fragmented, which limits the growth and coalescence of localized strain zones and delays crack initiation, leading to improved elongation.
While similar trends between microstructure and mechanical properties have been reported for Al–Si alloys [4, 17], different behaviors have been observed in other alloy systems. A more in-depth discussion on the underlying mechanisms governing microstructure–mechanical property relationships can be found in [19].

5. Conclusion

In this study, an experimental framework was applied to investigate the relationships among cooling rate, secondary dendrite arm spacing (SDAS), and mechanical properties in aluminum castings. Casting blocks with different thicknesses for obtaining wide range of cooling rates, and the use of the second derivative of cooling curves for identifying phase transformation regions were adopted based on established approaches reported in previous studies [13, 14]. Building upon these methods, this work focused on improving the experimental linkage between thermal history, microstructure, and mechanical properties.
The primary contribution of this study lies in the specimen extraction strategy. Due to inherent experimental constraints, it was not possible to extract both SDAS and tensile specimens from the exact thermocouple location. To address this issue, SDAS observation specimens were extracted from the thermocouple locations, while tensile specimens were extracted from symmetric positions with respect to the casting centerline, where identical thermal histories were assumed. This assumption was validated by comparing SDAS values measured at the symmetric locations, which showed good agreement. This approach enabled a consistent correlation between cooling rate, SDAS, and mechanical properties.
The relationship between SDAS and average cooling rate followed a power-law form, with a fitted exponent consistent with values reported in the literature [7], confirming the reliability of the thermal analysis. Tensile test results demonstrated that yield strength, ultimate tensile strength, and elongation increased with decreasing SDAS. Although some scatter was observed, particularly in elongation due to porosity and specimen geometry effects, consistent trends were obtained across all specimens.
Overall, the results confirm that SDAS is an effective microstructural parameter for describing the mechanical behavior of aluminum castings. The specimen extraction framework proposed in this study provides a practical and reliable methodology for experimentally correlating cooling conditions, dendritic microstructure, and mechanical properties, and can be readily extended to other casting alloys and solidification studies.

Acknowledgments

This work was supported by Basic Science Research Program through the National Research Foundation of Korea (NRF) funded by the Ministry of Education (RS-2025-25406725) and the InnoCORE program of the Ministry of Science and ICT (N10250154) and. This work is also partially supported by ARC Training Center of IC220100028.

References

[1] C.D. Lee, K.S Shin, Effects of precipitate and dendrite arm spacing on tensile properties and fracture behavior of as-cast magnesium-aluminum alloys, Met. Mater. Int. 9 (2003) 21–27.

[2] H. Cao, M. Wessén, Effect of microstructure on mechanical properties of as-cast Mg-Al alloys, Metall. Mater. Trans. A-Phys. Metall. Mater. Sci. 35 (2004) 309–319

[3] M. Okayasu, K. Ota, S. Takeuchi, H. Ohfuji, T. Shiraishi, Influence of microstructural characteristics on mechanical properties of ADC12 aluminum alloy, Mater. Sci. Eng. A-Struct. Mater. Prop. Microstruct. Process. 592 (2014) 189-200.

[4] M. Wierzbińska, J. Sieniawski, Effect of dendrite arm spacing on cleavage fracture toughness of Al–5Si–1Cu alloy, Int. J. Cast. Metals Res. 17.5 (2004) 267-270.

[5] M.Ş. Turhal, T. Savaşkan, Relationships between secondary dendrite arm spacing and mechanical properties of Zn-40Al-Cu alloys, J. Mater. Sci. 38 (2003) 2639–2646.

[6] G.A. Santos, C. de Moura Neto, W.R. Osório, A. Garcia, Design of mechanical properties of a Zn27Al alloy based on microstructure dendritic array spacing, Mater. Des. 28.9 (2007) 2425-2430.

[7] M.C. Flemings, Solidification Processing, McGraw-Hill, 1974, Chapter 5.

[8] R. Chen, Y. Shi, Q. Xu, B. Liu, Effect of cooling rate on solidification parameters and microstructure of Al-7Si-0.3Mg-0.15Fe alloy, Transactions of Nonferroues Metals Society of China 24.6 (2014) 1645-1652.

[9] Y. Ding, J.A. Muñiz-Lerma, M. Trask, S. Chou, A. Walker, M. Brochu, Microstructure and mechanical property considerations in additive manufacturing of aluminum alloys, MRS Bull. 41 (2016), 745-751.

[10] M.O. Shabani, A. Mazahery, Prediction of mechanical properties of cast A356 alloy as a function of microstructure and cooling rate. Arch. Metall. Mater. 56.3 (2011) 671-675.

[11] H. Tang, Q. Wang, C. Lei, B. Ye, K. Wang, H. Jiang, W. Ding, X. Zhang, Z. Lin, J. Zhang, Effect of cooling rate on microstructure and mechanical properties of an Al-5.0 Mg-3.0 Zn-1.0 Cu cast alloy. J. Alloy. Compd. 801 (2019) 596-608.

[12] M. J. Behnam, P. Davami, N. Varahram, Effect of cooling rate on microstructure and mechanical properties of gray cast iron. Mater. Sci. Eng. A-Struct. Mater. Prop. Microstruct. Process. 528.2 (2010) 583-588.

[13] D.M. Stefanescu, Thermal analysis—theory and applications in metalcasting. Int. J. Met. 9:1 (2015) 7-22.

[14] G. Alonso, P. Larrañaga, J. Sertucha, R. Suárez, Gray cast iron with high austenite-to-eutectic ratio part I – calculation and experimental evaluation of the fraction of primary austenite in cast iron, Trans. AFS, 120 (2012) 329-335.

[15] G.A. Chadwick, Metallography of phase transformations, Butterworth, 1974, 107-147.

[16] L.E. Ramirez-Vidaurri, M. Castro-Roman, M. Herrera-Trejo, K.L. Fraga-Chavez, Secondary dendritic arm spacing and cooling rate relationship for an ASTM F75 alloy, J. Mater. Res. Technol-JMRT 19 (2022) 5049-5065.

[17] P.R. Goulart, J.E. Spinelli, W.R. Osório, A. Garcia, Mechanical properties as a function of microstructure and solidification thermal variables of Al–Si castings, Mater. Sci. Eng. A-Struct. Mater. Prop. Microstruct. Process. 421.1-2 (2006) 245-253.

[18] G. Sigworth, Fundamentals of solidification in aluminum castings. Int. J. Metalcast. 8.1 (2014) 7–20.

[19] S. Liu, G. Huang, M. Gupta, B. Jiang, F. Pan, Microstructures, mechanical properties and deformation mechanism of heterogeneous metal materials: A review, J. Mater. Sci. Technol. 248 (2026) 1-46.